

Supporting Information

Macrocycle-assisted synthesis of non-stoichiometric silver(I) halide electrocatalysts for efficient chlorine evolution reaction

Qiong-You Zhang, Xin He, and Liang Zhao*

The Key Laboratory of Bioorganic Phosphorus Chemistry & Chemical Biology (Ministry of Education), Department of Chemistry, Tsinghua University, Beijing 100084, China

zhaolchem@mail.tsinghua.edu.cn

X-ray Crystallographic Analysis

Crystal data for $[\text{Ag}_4\text{Cl}(\text{CF}_3\text{SO}_3)_3(\text{Py}[7])](\text{CH}_3\text{OH})$ (**1**, CCDC-1527294): $\text{C}_{46}\text{H}_{46}\text{Ag}_4\text{ClF}_9\text{N}_{14}\text{O}_{10}\text{S}_3$, $M = 1689.08$, monoclinic, space group $P2_1/n$ (No. 14), $a = 24.864(5) \text{ \AA}$, $b = 10.112(2) \text{ \AA}$, $c = 24.940(5) \text{ \AA}$, $\beta = 114.19(3)^\circ$, $V = 5720(2) \text{ \AA}^3$, $Z = 4$, $T = 173 \text{ K}$, $D_c = 1.961 \text{ g cm}^{-3}$. The structure, refined on F^2 , converged for 9994 unique reflections ($R_{\text{int}} = 0.0643$) and 8482 observed reflections with $I > 2\sigma(I)$ to give $R_1 = 0.0962$ and $wR_2 = 0.1894$ and a goodness-of-fit = 1.225. Silver atom Ag2 is disordered at two separated positions with a refined occupancy ratio of 0.89:0.11.

Crystal data for $[\text{Ag}_5\text{Br}(\text{CF}_3\text{SO}_3)_2(\text{H}_2\text{O})_4(\text{Py}[7])](\text{CF}_3\text{SO}_3)_2 \cdot \text{H}_2\text{O}$ (**2**, CCDC-1527295): $\text{C}_{46}\text{H}_{52}\text{Ag}_5\text{BrF}_{12}\text{N}_{14}\text{O}_{17}\text{S}_4$, $M = 2048.52$, triclinic, space group $P-1$ (No. 2), $a = 10.277(2) \text{ \AA}$, $b = 17.015(3) \text{ \AA}$, $c = 19.143(4) \text{ \AA}$, $\alpha = 91.21(3)^\circ$, $\beta = 102.96(3)^\circ$, $\gamma = 90.15(3)^\circ$, $V = 3261.4(11) \text{ \AA}^3$, $Z = 2$, $T = 173 \text{ K}$, $D_c = 2.086 \text{ g cm}^{-3}$. The structure, refined on F^2 , converged for 14837 unique reflections ($R_{\text{int}} = 0.0442$) and 13437 observed reflections with $I > 2\sigma(I)$ to give $R_1 = 0.0442$ and $wR_2 = 0.1083$ and a goodness-of-fit = 1.068. Silver atom Ag2 is disordered at two positions with a refined occupancy ratio of 0.70:0.30. The triflate anion S4 has two orientational disorder positions with a refined occupancy ratio of 0.72:0.28.

Crystal data for $[\text{Ag}_4\text{I}(\text{H}_2\text{O})_2(\text{Py}[7])](\text{CF}_3\text{SO}_3)_3$ (**3**, CCDC-1527296): $\text{C}_{45}\text{H}_{42}\text{Ag}_4\text{F}_9\text{IN}_{14}\text{O}_{10}\text{S}_3$, $M = 1764.49$, orthorhombic, space group $Pnma$ (No. 62), $a = 26.256(5) \text{ \AA}$, $b = 21.160(4) \text{ \AA}$, $c = 10.086(2) \text{ \AA}$, $V = 5603.6(19) \text{ \AA}^3$, $Z = 4$, $T = 173 \text{ K}$, $D_c = 2.092 \text{ g cm}^{-3}$. The structure, refined on F^2 , converged for 5068 unique reflections ($R_{\text{int}} = 0.0646$) and 4328 observed reflections with $I > 2\sigma(I)$ to give $R_1 = 0.0835$ and $wR_2 = 0.1439$ and a goodness-of-fit = 1.209. Silver atom Ag3 is disordered at three separated positions with a refined occupancy ratio of 0.36:0.32:0.32. The triflate anion S2 has two orientational disorder positions with a refined occupancy ratio of 0.52:0.48. A disordered atom C24 was refined isotropically.

Supporting Figures

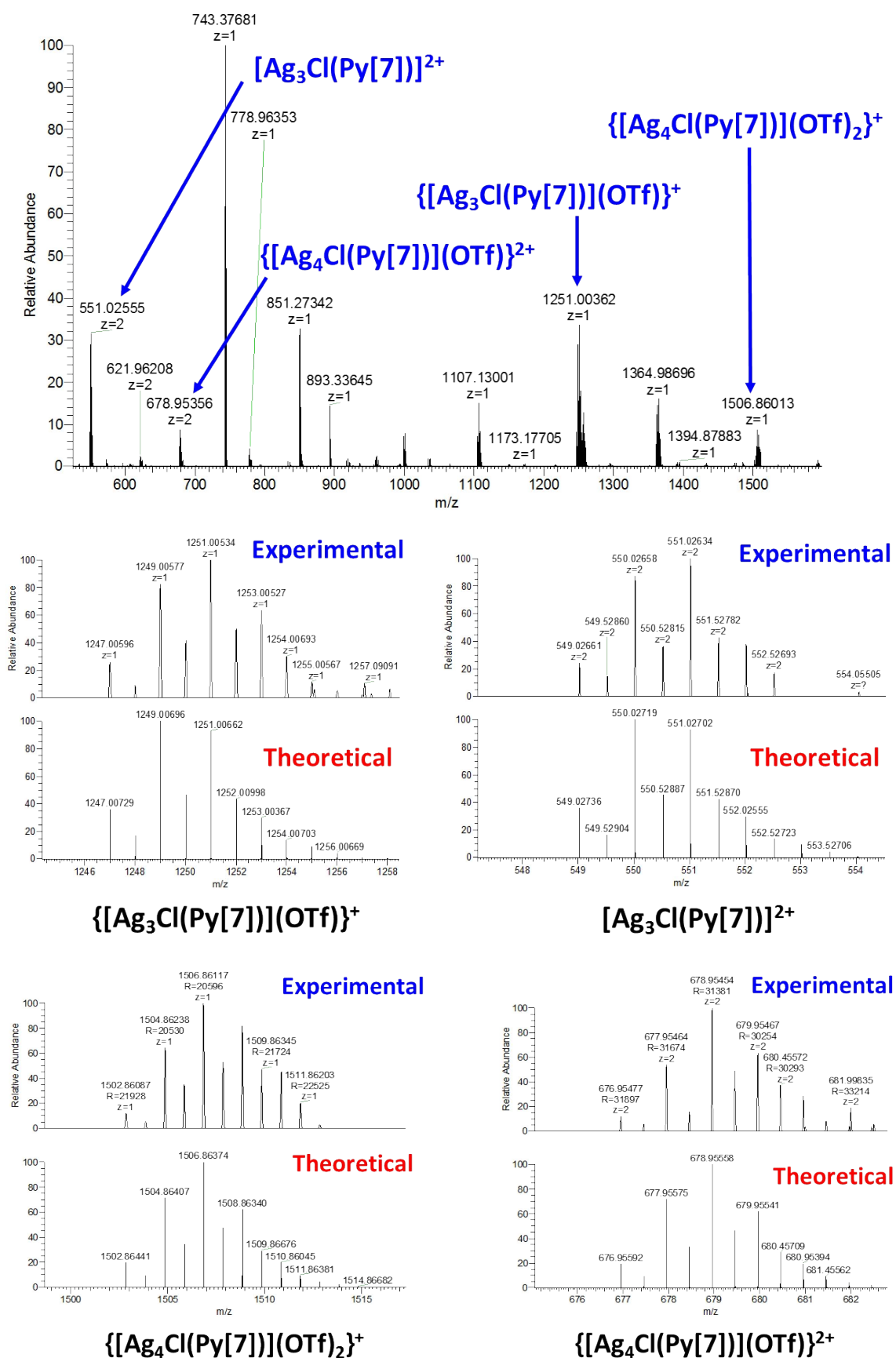


Fig. S1 High resolution ESI-MS spectra of complex 1.

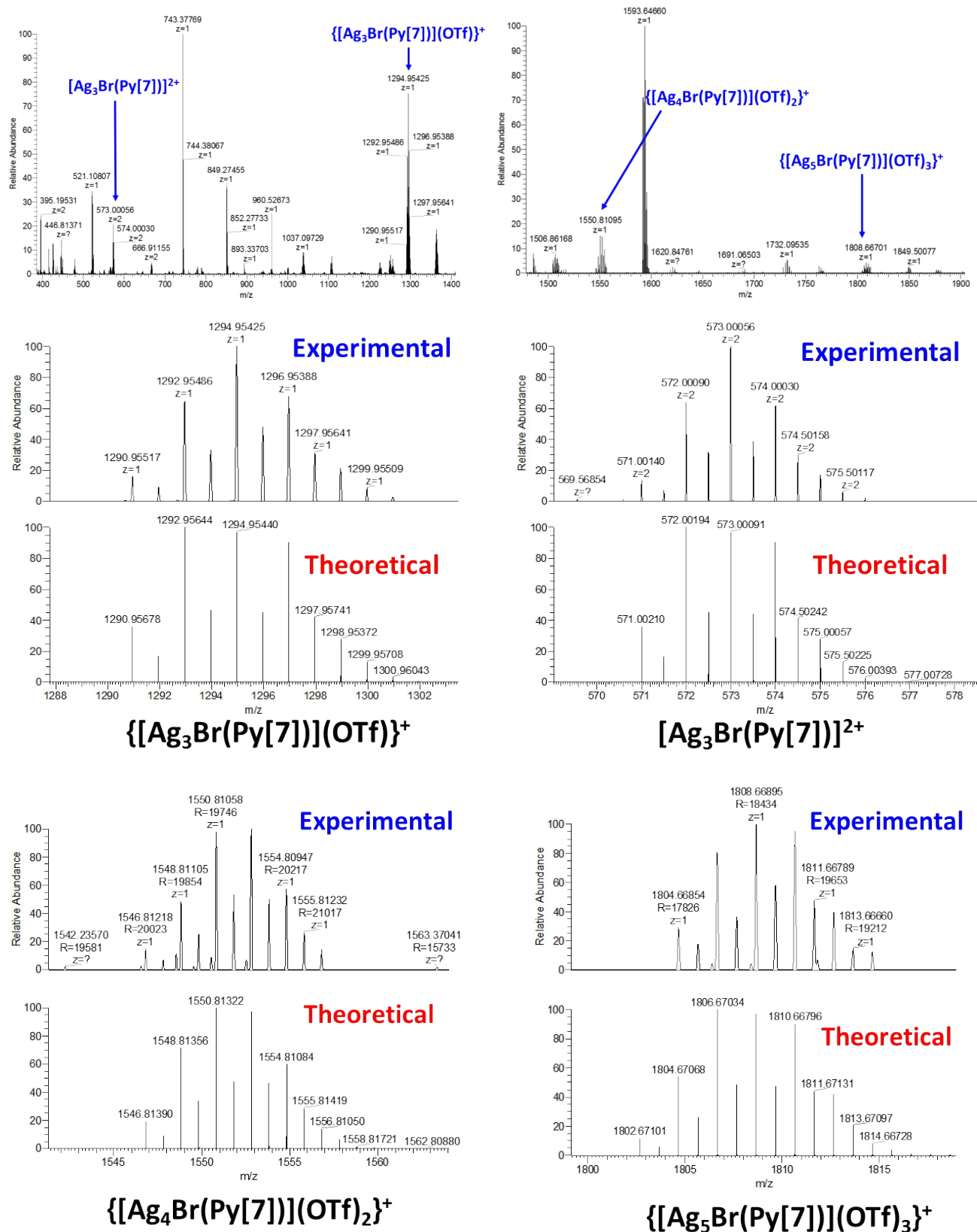


Fig. S2 High resolution ESI-MS spectra of complex 2.

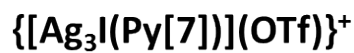
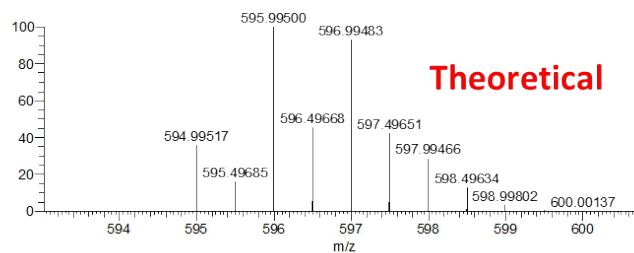
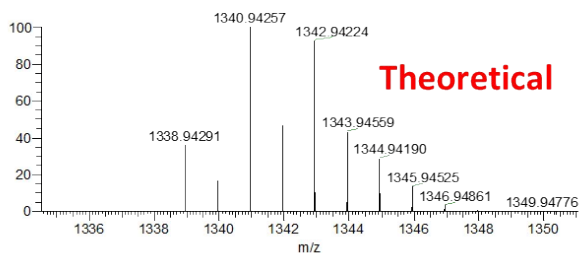
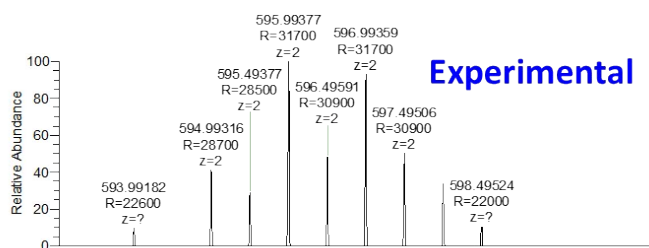
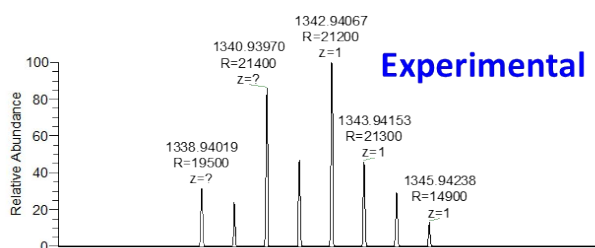
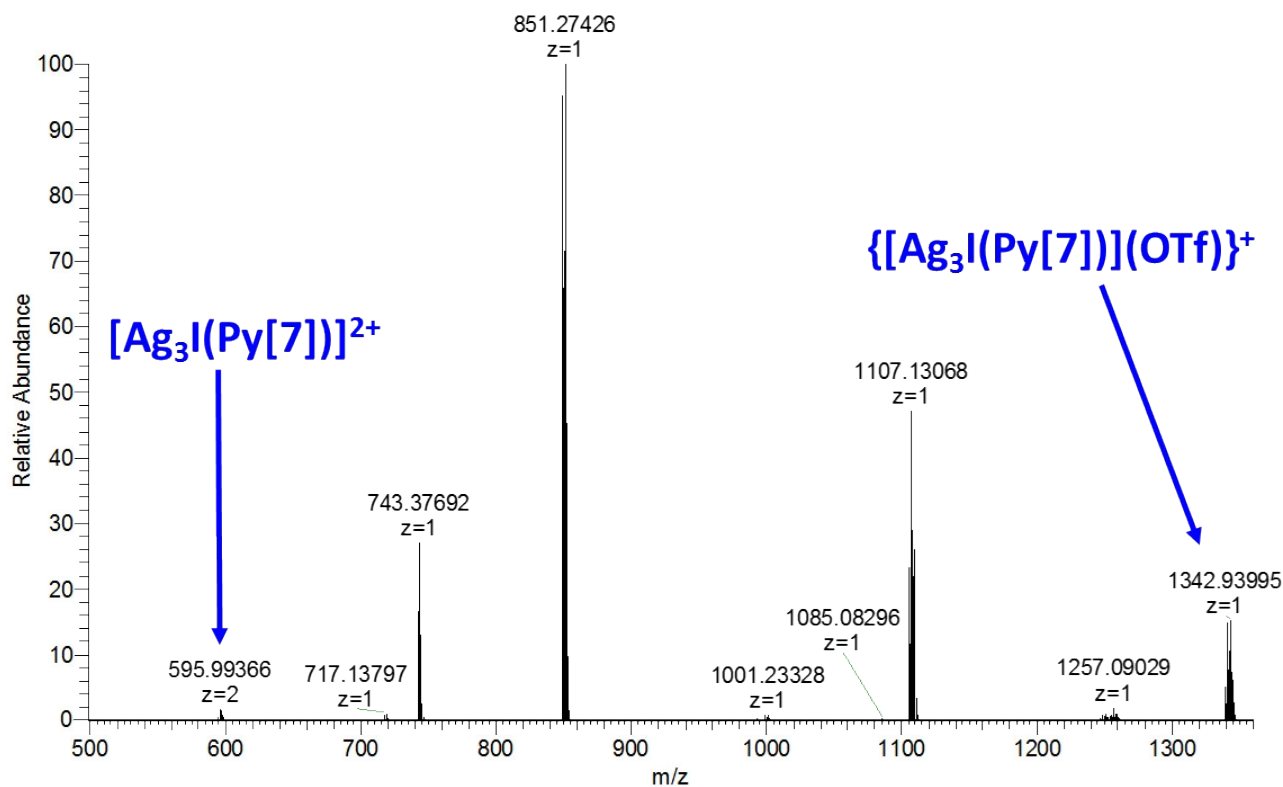


Fig. S3 High resolution ESI-MS spectra of complex 3.

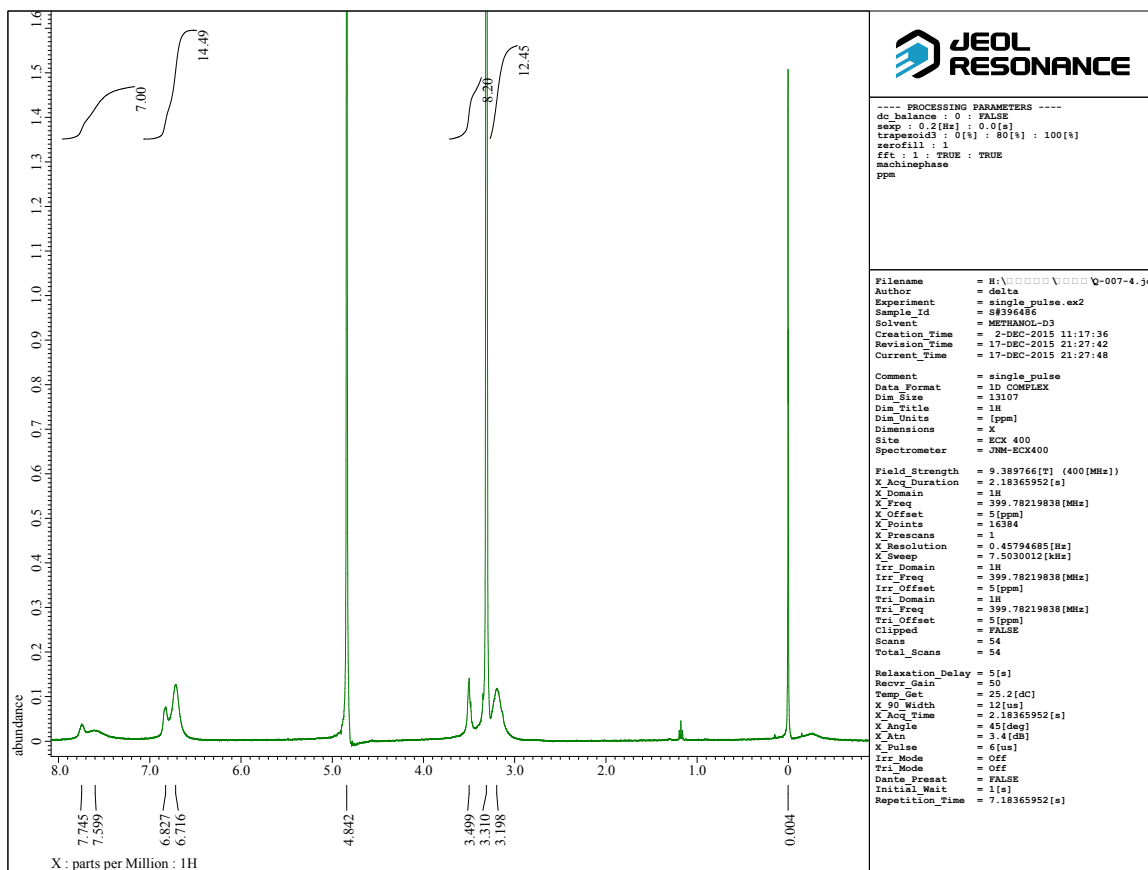


Fig. S4 $^1\text{H-NMR}$ spectrum (400MHz, methanol- d_4 : CDCl_3 , ν : $\nu = 1 : 1$) of complex 1.

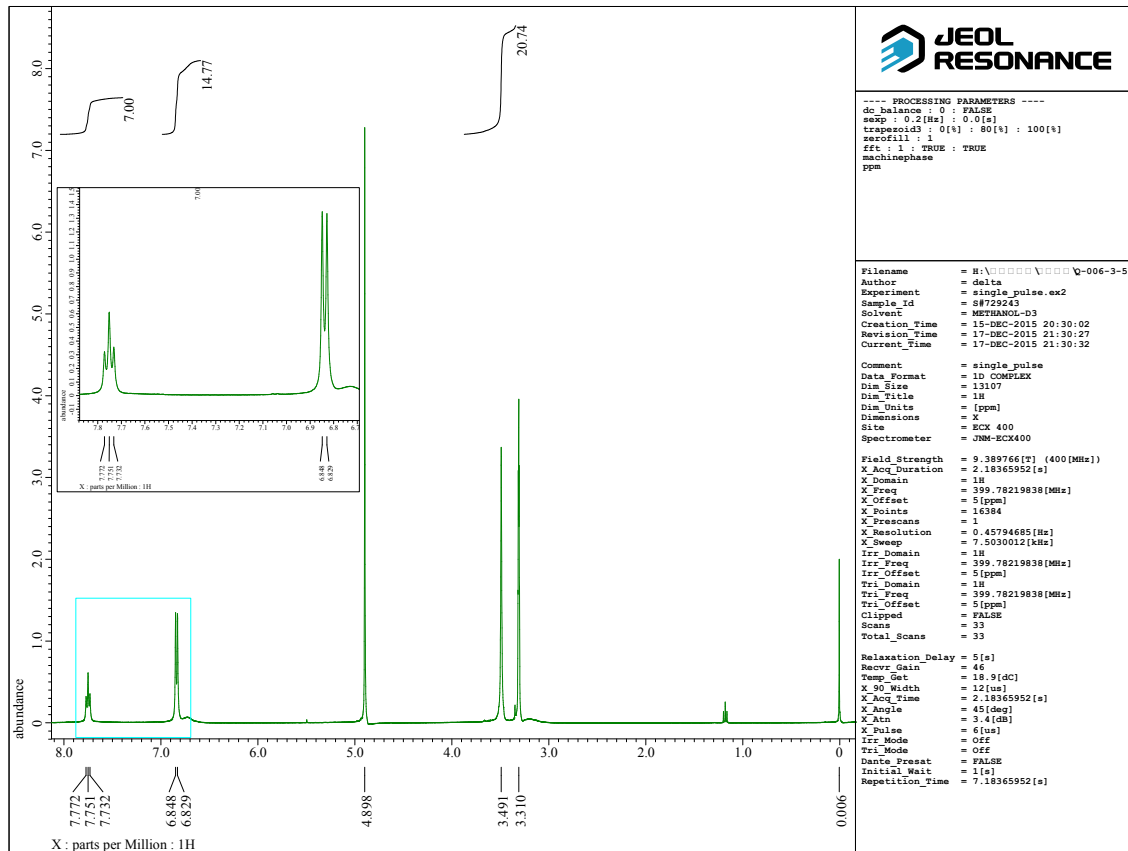


Fig. S5 $^1\text{H-NMR}$ spectrum (400MHz, methanol- d_4 : CDCl_3 , ν : $\nu = 1 : 1$) of complex 2.

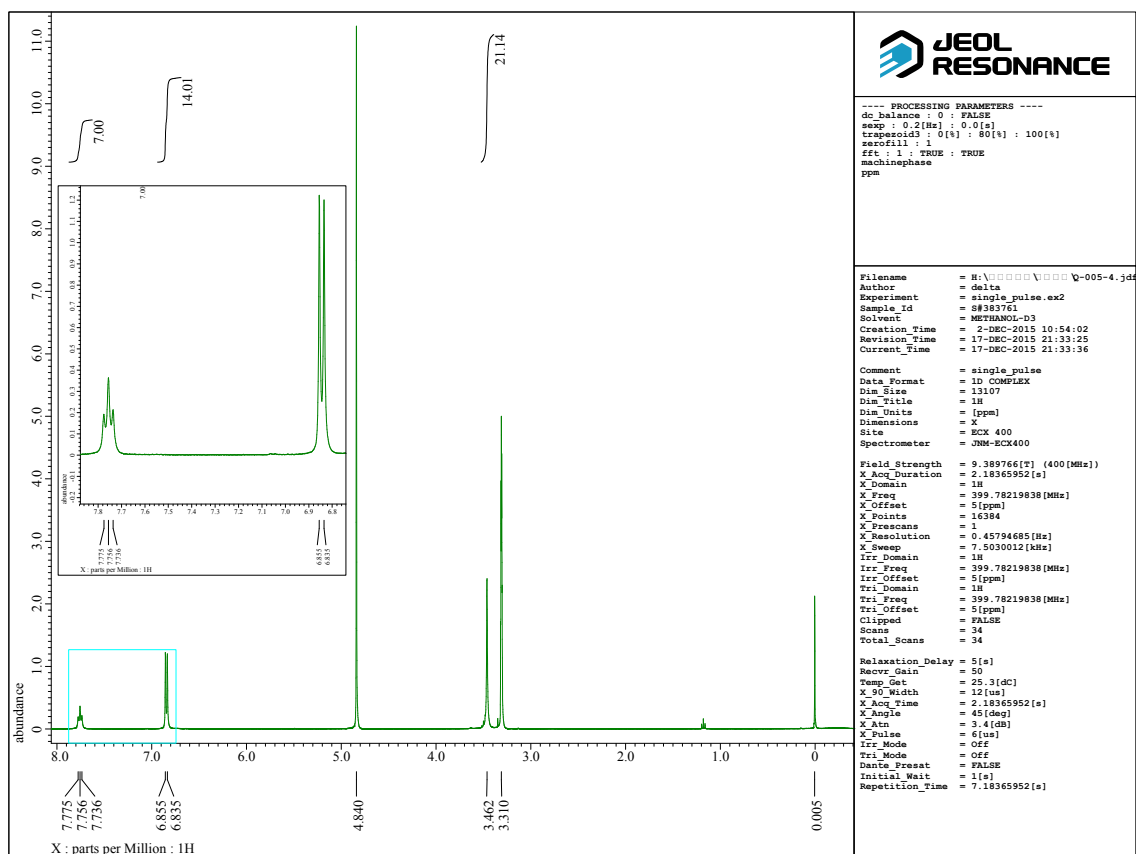


Fig. S6 ^1H -NMR spectrum (400MHz, methanol- d_4 : CDCl_3 , $v : v = 1 : 1$) of complex **3**.

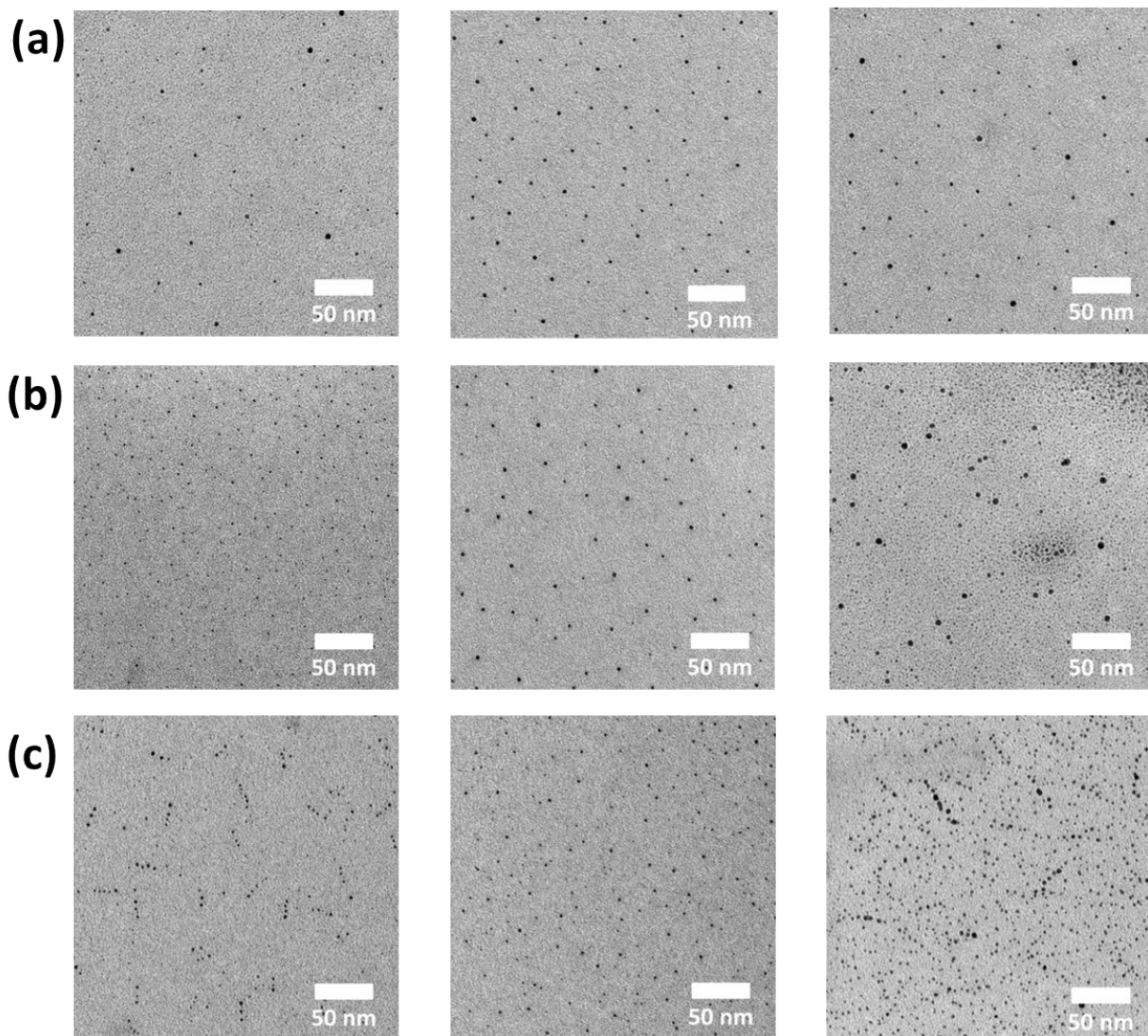


Fig. S7 TEM images for the stepwise growth of nanometer-sized particles upon adding HBF_4 into the solution of (a) complex **1**, (b) complex **2**, (c) complex **3**. From left to right: after 1, 2 and 3 minutes.

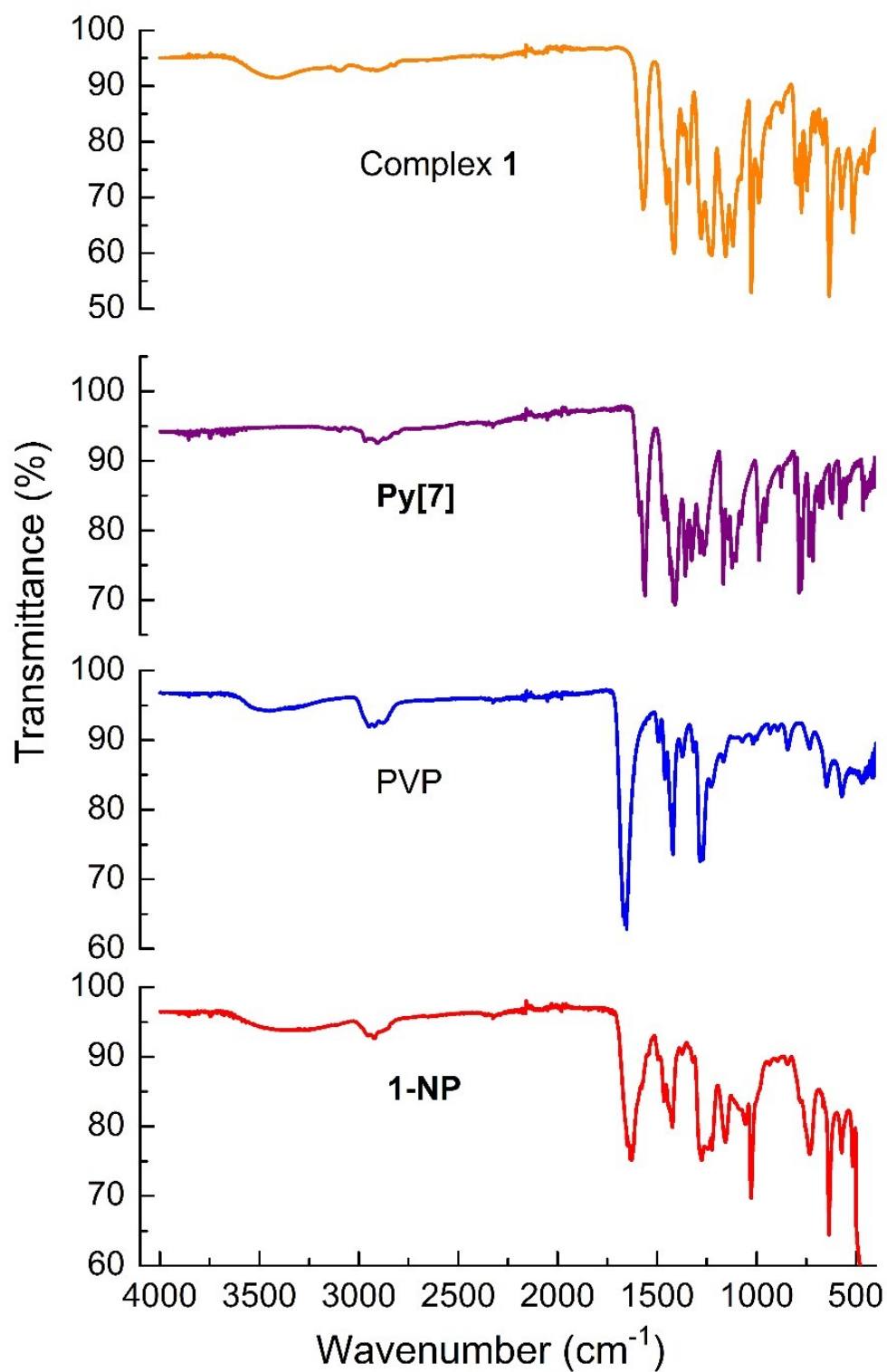


Fig. S8 FT-IR spectra of 1-NP, PVP, macrocyclic ligand Py[7] and complex 1.

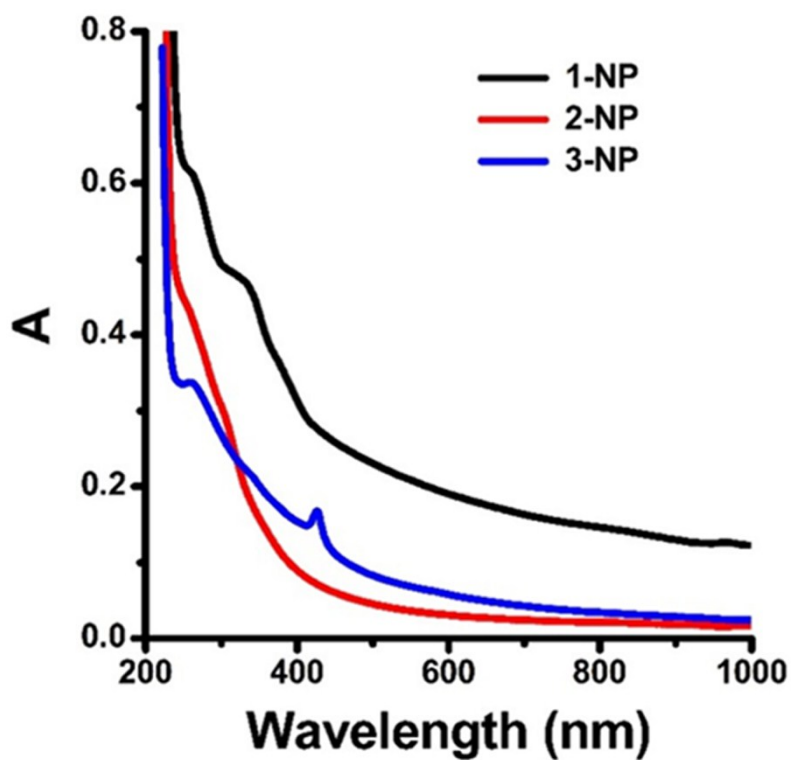


Fig. S9 UV-vis spectra of 1- to 3-NP in methanol at 298 K.

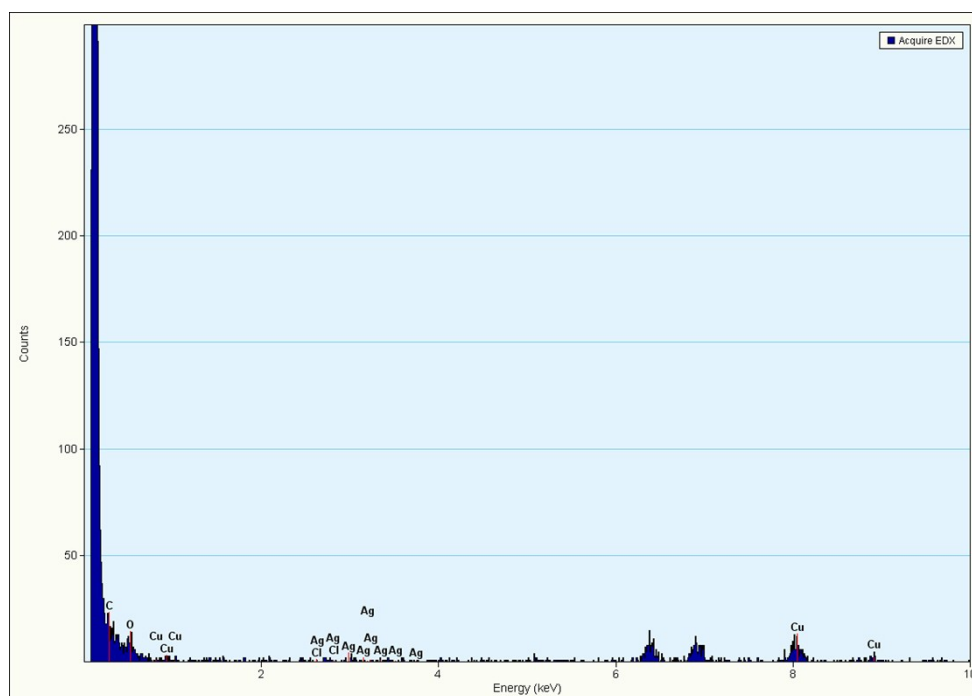


Fig. S10 EDX spectrum of 1-NP. The Ag/Cl ratio was determined as 4.6 based on the atomic ratio of Ag-82.3% and Cl-17.7%.

Element	Weight %	Atomic %	Uncert. %	Correction	k-Factor
Cl(K)	6.60	17.71	4.65	0.95	1.063
Ag(K)	93.39	82.28	42.56	0.98	6.491

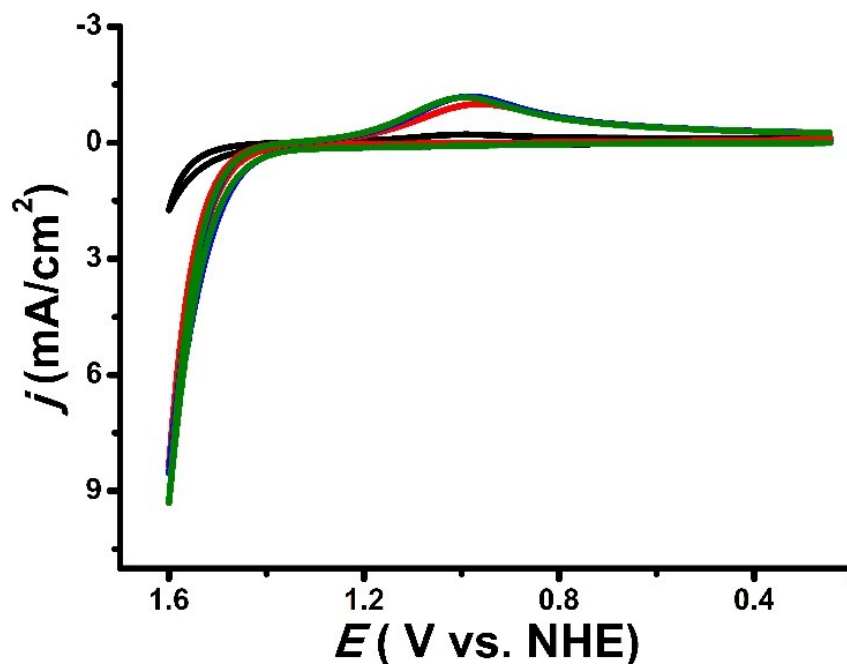


Fig. S11 CVs at a GC electrode (0.071 cm^2) in an aqueous solution of NaCl (1 M) and HNO_3 (pH ~ 1 , 0.1 M) without (black) and with (red) 2-NP ($c_{\text{Ag}^+} = 5.04 \text{ }\mu\text{M}$) and (green) 3-NP ($c_{\text{Ag}^+} = 6.72 \text{ }\mu\text{M}$). Scan rate: 100 mV/s.

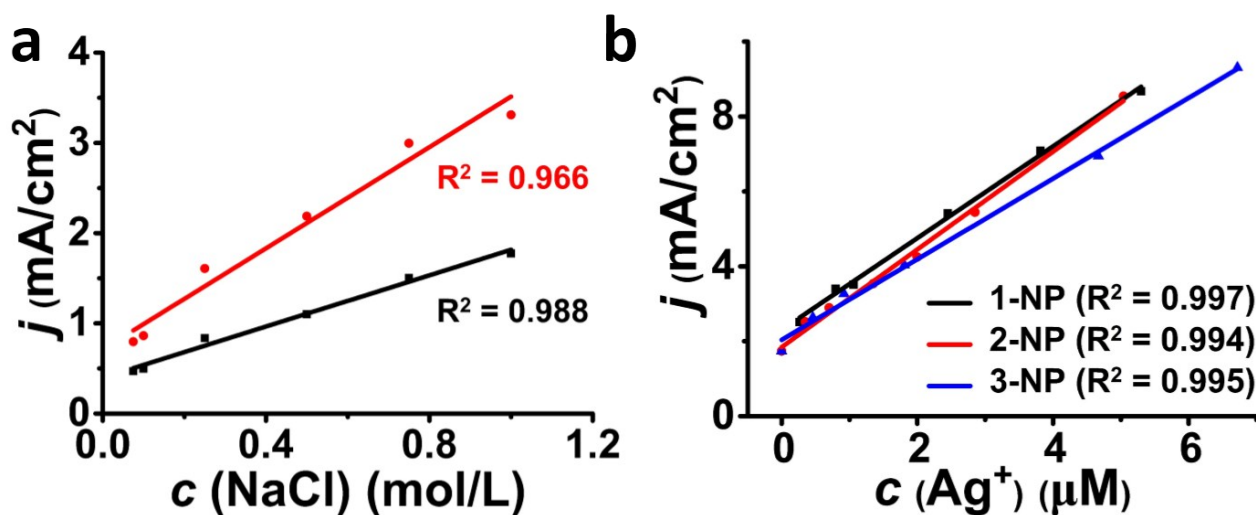


Fig. S12 (a) Plot of catalytic current density vs. NaCl concentration in 0.1 M HNO_3 solution without (black) and with (red) 1-NP ($c_{\text{Ag}^+} = 0.53 \text{ }\mu\text{M}$). (b) Plot of catalytic current density vs. silver(I) concentration of 1-3-NP (1 M NaCl, 0.1 M HNO_3).

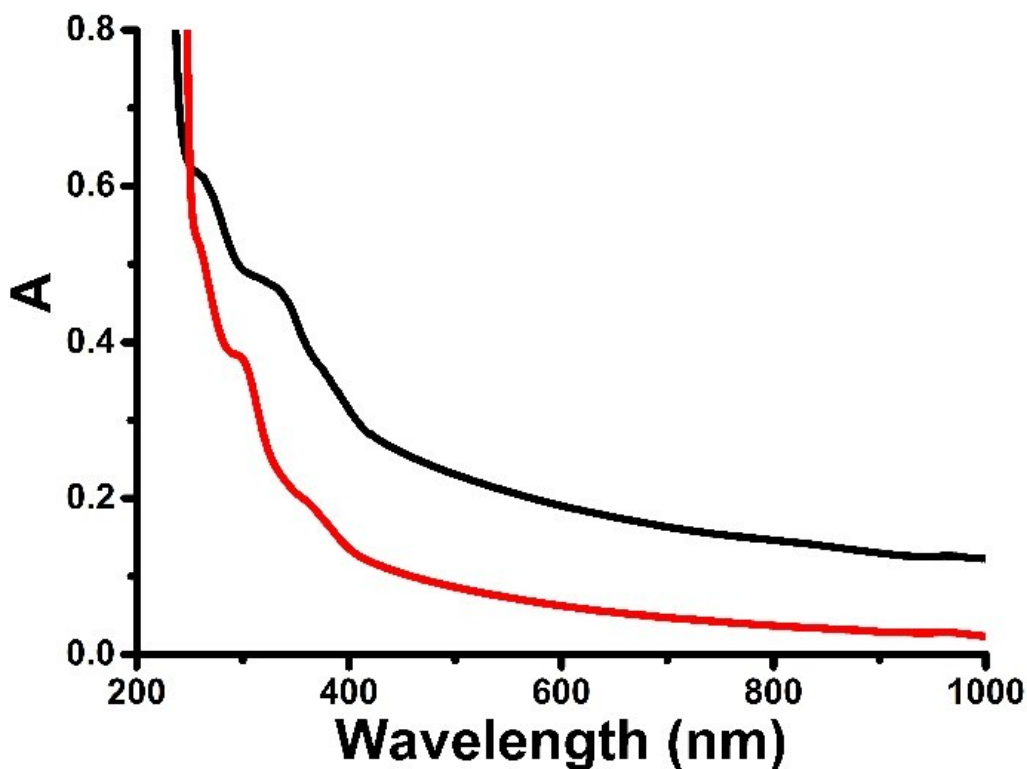


Fig. S13 UV-vis spectra of 1-NP in (black) H₂O and (red) in an aqueous solution of NaCl (1 M) and HNO₃ (0.1 M) at 298 K.

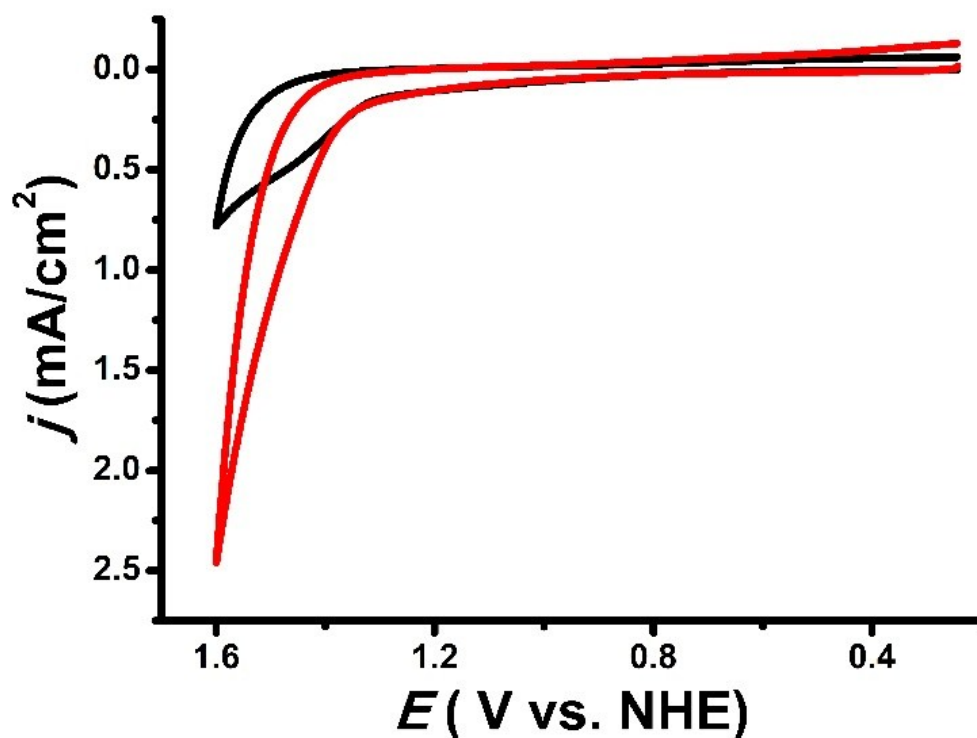


Fig. S14 CVs of a glassy carbon electrode (0.071 cm²) in a NaH₂PO₄/Na₂HPO₄ buffer solution (0.1 M, pH~7) of NaCl (0.55 M) without (black) and with (red) 1-NP (c_{Ag⁺} = 0.53 μM). Scan rate: 100 mV/s.

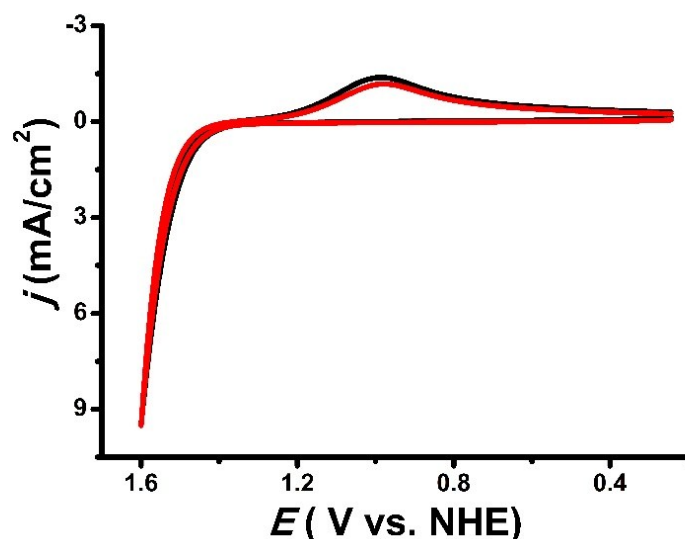


Fig. S15 CVs of a glassy carbon electrode (0.071 cm^2) in an aqueous solution of NaCl (1 M) and HNO_3 (pH ~ 1 , 0.1 M) with **1-NP** ($c_{\text{Ag}^+} = 5.30 \text{ } \mu\text{M}$) (black) before and (red) after electrolysis.

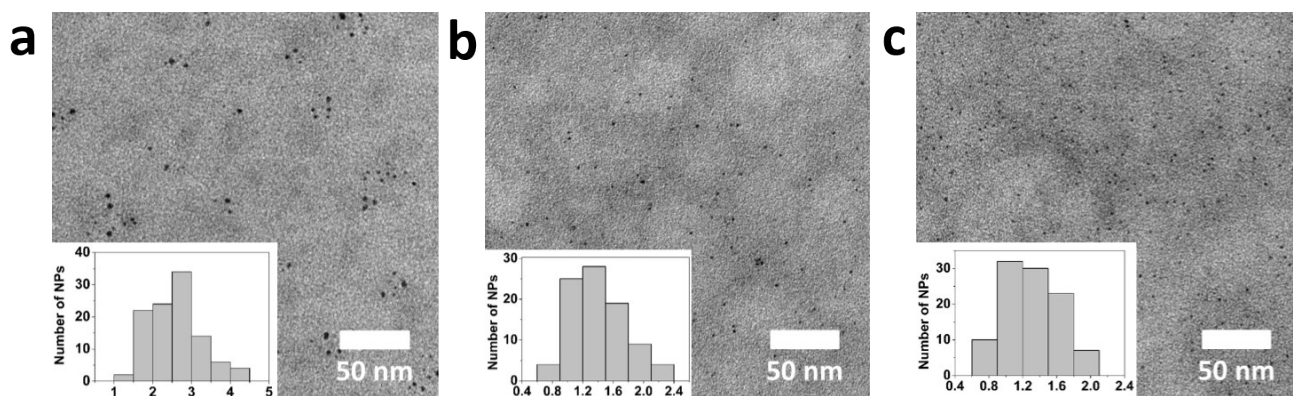


Fig. S16 TEM images and size-distribution histograms of (a) **1-NP** ($2.5 \pm 1.5 \text{ nm}$) in 0.05 M NaCl aqueous solution, (b) **2-NP** ($1.5 \pm 0.9 \text{ nm}$) in 1 M NaCl aqueous solution, and (c) **3-NP** ($1.4 \pm 0.7 \text{ nm}$) in 1 M NaCl aqueous solution.

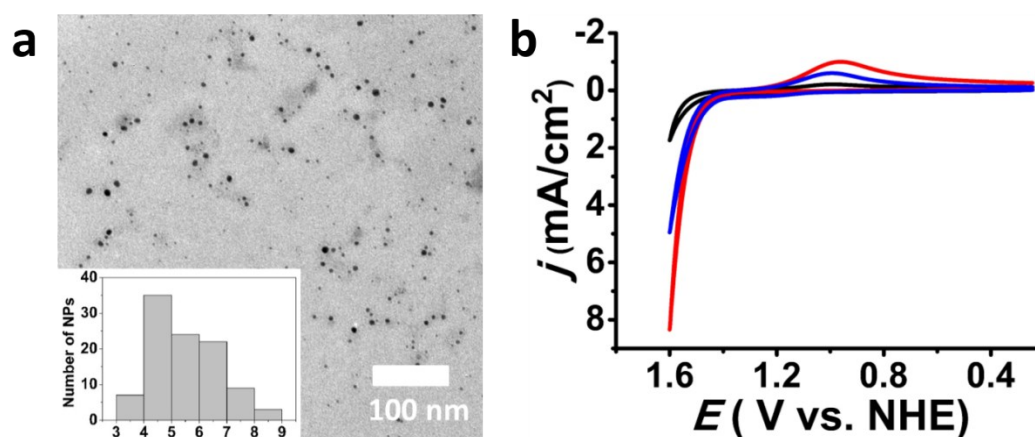


Fig. S17 (a) TEM image and size-distribution histogram of **1-NP** in larger sizes ($6.0 \pm 3.0 \text{ nm}$). (b) CVs at a GC electrode in an aqueous solution of NaCl (1 M) and HNO_3 (pH ~ 1 , 0.1 M) without (black) and with **1-NP** in $2.5 \pm 1.5 \text{ nm}$ (red) and $6.0 \pm 3.0 \text{ nm}$ (blue). Scan rate: 100 mV/s.

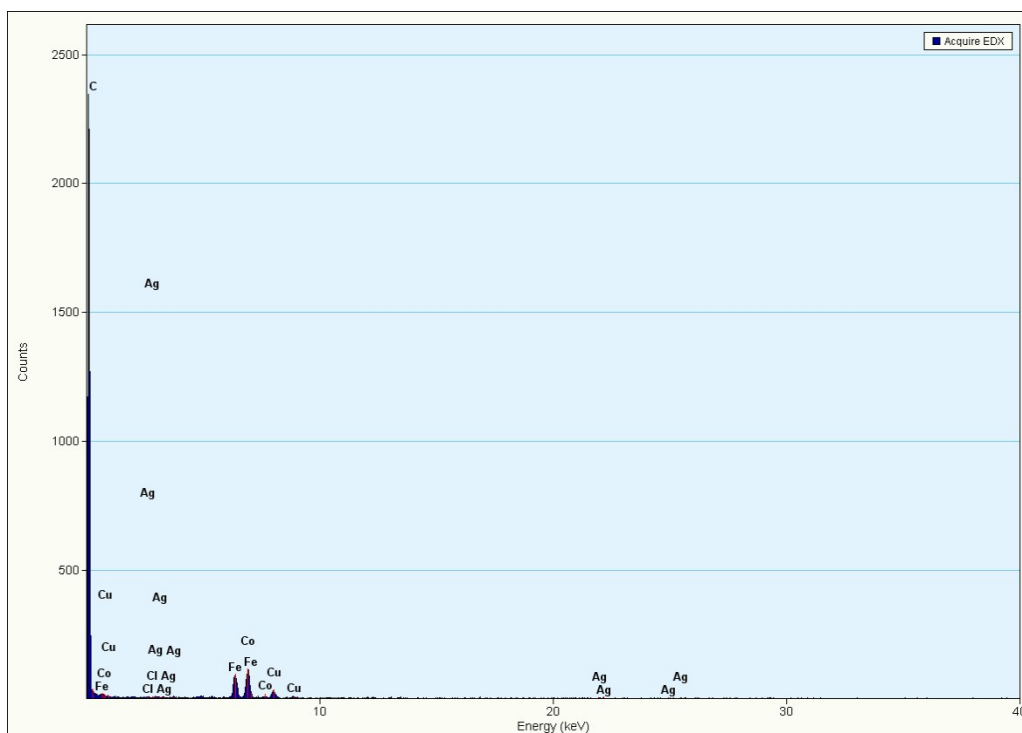


Fig. S18 EDX spectrum of **1-NP** in 1M NaCl solution . The Ag/Cl ratio was determined as 1.1 based on the atomic ratio of Ag-51.9% and Cl-48.1%.

Element	Weight %	Atomic %	Uncert. %	Correction	k-Factor
Cl(K)	23.34	48.08	13.90	0.95	1.063
Ag(L)	76.65	51.91	38.48	0.95	2.617

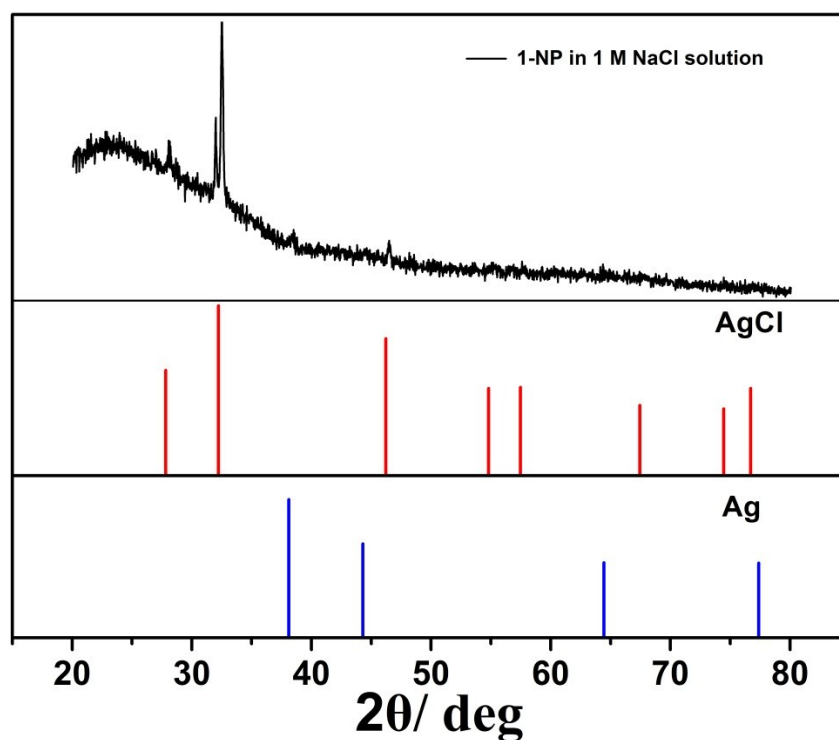


Fig. S19 XRD patterns of **1-NP** in 1M NaCl solution and the reference AgCl (JCPDS file: 31-1238) and Ag (JCPDS file: 87-0597).

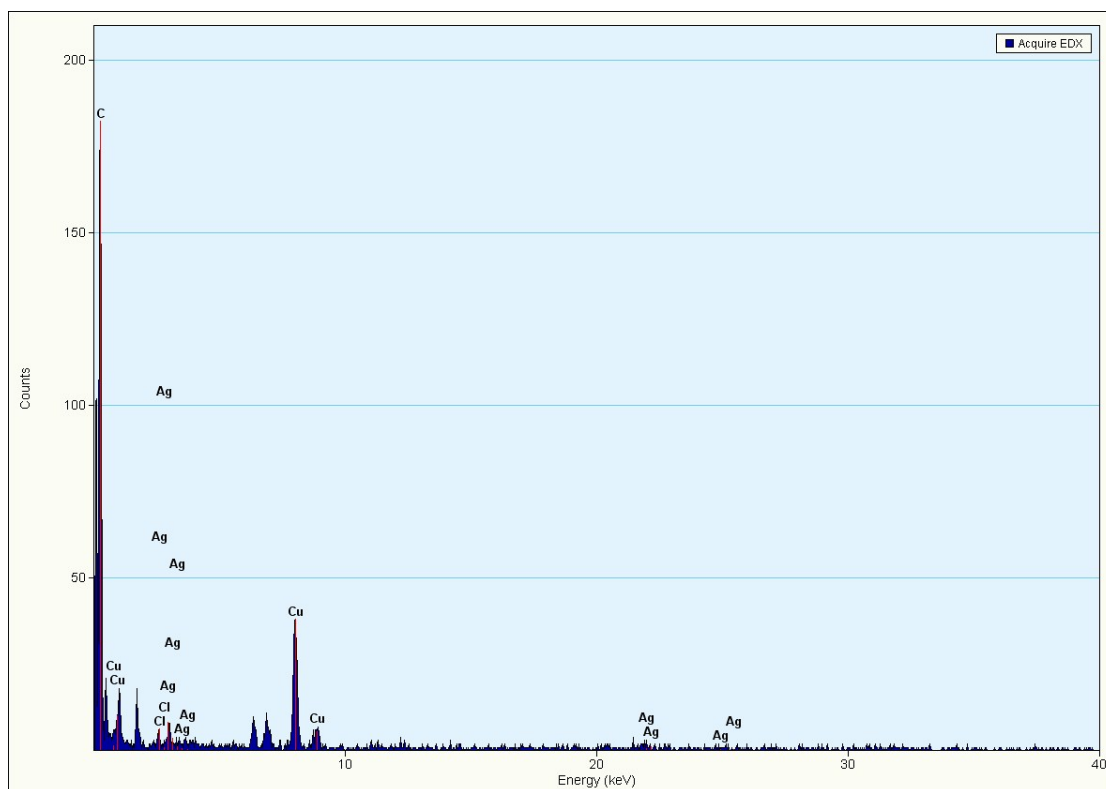


Fig. S20 EDX spectrum of **1-NP** in 1M NaCl solution after 1h controlled potential electrolysis. The Ag/Cl ratio was determined as 3.7 based on the atomic ratio of Ag-78.8% and Cl-21.2%.

Element	Weight %	Atomic %	Uncert. %	Correction	k-Factor
Cl(K)	8.12	21.20	7.27	0.95	1.063
Ag(L)	91.87	78.79	20.42	0.95	2.617

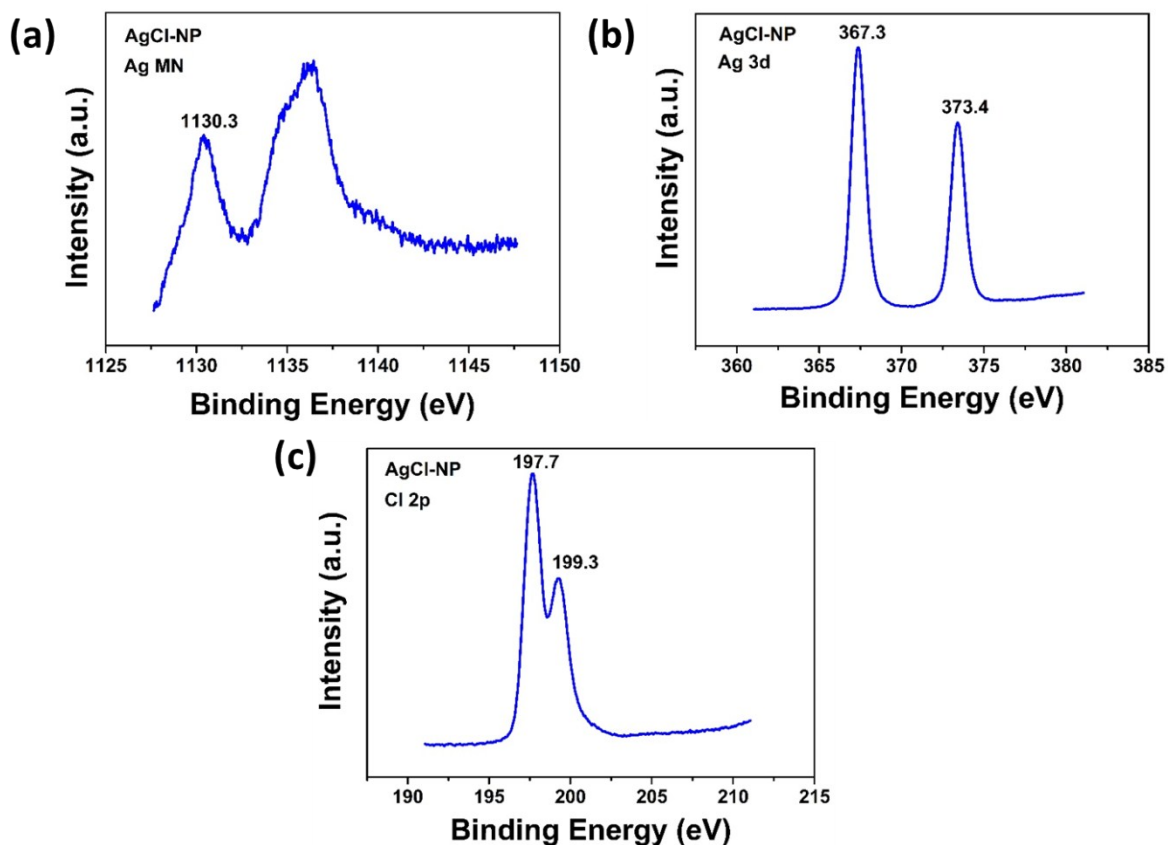


Fig. S21 Ag MN, Ag 3d and Cl 2p signals for the PVP-stabilized stoichiometric AgCl nanoparticles AgCl-NP (C. An, S. Peng and Y. Sun, *Adv. Mater.*, 2010, **22**, 2570-2574). The Ag MN signals were determined by AES while the binding energies for Ag 3d and Cl 2p were measured by XPS. The +1 oxidation state of silver was determined based on the Ag 3d^{5/2} and Ag 3d^{3/2} binding energy peaks at 373.4 and 367.3 eV, respectively.